



## Adsorption, thermodynamic and quantum chemical studies of 3-(4-Chlorobenzoylmethyl)benzimidazoliumbromide in inhibition effect on carbon steel

P. Kannan<sup>a</sup>, S. K. Shukla<sup>b</sup>, T. S. Rao<sup>b</sup>, N. Rajendran<sup>a\*</sup>

<sup>a</sup> Department of Chemistry, Anna University, Chennai-600025, Tamil Nadu, India

<sup>b</sup> Biofouling and Biofilm Processes Section, Water and Steam Chemistry Division, Bhabha Atomic Research Centre, Kalpakkam-603102, Tamil Nadu, India.

Received 29 May 2015, Revised 08 Jan 2016, Accepted 20 Jan 2016

\*Corresponding author: E-mail: [nrajendran@annauniv.edu](mailto:nrajendran@annauniv.edu); Phone: (+91-44-22358659)

### Abstract

The corrosion inhibition efficiency of 3-(4-chlorobenzoylmethyl) benzimidazoliumbromide in water medium has been evaluated using electrochemical and other techniques. The mixed type inhibitive behavior of the inhibitor was evaluated by potentiodynamic polarization study. The inhibition efficiency increased with increasing pH up to 7.0 and showed a decrease with rise in temperature of the medium. Charge transfer resistance ( $R_{ct}$ ) values confirmed the formation of a protective layer by the adsorption of the inhibitor on the carbon steel surface. The adsorption degree of 3-(4-chlorobenzoylmethyl) benzimidazoliumbromide on the metal substrate obeyed Langmuir adsorption isotherms. Surface characterization of the carbon steel in the absence and presence of inhibitor has been monitored by atomic force (AFM) and scanning electron microscopy (SEM) with energy dispersive X-Ray spectroscopy (EDX). Quantum chemical analysis (QCA) data supported the adsorption efficiency of the inhibitor. The results obtained from electrochemical noise analysis (ENA) were in good agreement with other studies.

**Keywords:** Inhibitor, ENA, Atomic force microscope, SEM/EDX, QCA.

### 1. Introduction

All over the world, carbon steel is mainly used as a structural material [1] in industries for many years. Corrosion is the most frequently encountered problem in the usage of carbon steel resulting in hampering the production in the industries besides huge economic loss. This necessitates finding out a suitable solution to overcome the situation. Of the all the methods available to mitigate corrosion, the use of corrosion inhibitors play a prominent role in effectively facing the situation. The main trend in the investigation of inhibitors is the study of corrosion prevention, antifouling, anti scale formation, etc. Organic substances containing nitrogen, oxygen and sulphur atoms are known to be proven corrosion inhibitors [2]. Many organic inhibitors such as azole [3], monosaccharide [4], carboxylic acid [5], polymer [6] and inorganic inhibitors like sodium nitrate [7], sodium gluconate [8], phosphate [9] and molybdate [10] quaternary salt [11] are being used in water medium at different conditions for prevention of corrosion. Out of these countless inhibitors, ionic liquids are the new novel class of corrosion inhibitors for a variety of metals in the recent past [12, 13]. Ionic liquids are molten salts that consist of cations and anions. Generally the cationic part behaves as active centre for adsorption and it contains hetero atom and  $\pi$ - electron system. Mostly, imidazolium [14-17] and pyridinium [18-20] based ionic liquids are used for corrosion prevention. Carbon steels used in many water distribution systems, effortlessly get corroded in their structure. Corrosion products could settle down throughout the entire path and will disturb the distribution and therefore the situation warrants for the elimination of corrosion products. In the present study, benzimidazole based ionic liquid namely, 3-(4-chlorobenzoylmethyl) benzimidazoliumbromide was

characterized for the prevention of carbon steel corrosion. Various concentrations of 3-(4-chlorobenzoylmethyl) benzimidazoliumbromide in water medium have been investigated to check the corrosion of carbon steel. Due to its unique properties such as, non flammability, very low vapor pressure, boiling and melting point, it has several advantages over others and hence considered as a green corrosion inhibitor. Moreover, inhibitor with high molecular surface area will ensure better protection by offering large surface coverage. Electrochemical studies were used to study the corrosion phenomenon. Thermodynamic, kinetic parameters and surface topology at various concentrations of 3-(4-chlorobenzoylmethyl) benzimidazoliumbromide on carbon steel were also examined and discussed.

## 2. Materials and Methods

### 2.1. Materials

To study the inhibition effect of 3-(4-chlorobenzoylmethyl) benzimidazoliumbromide on ASTM A53 grade carbon steel samples were used. Chemical composition of carbon steel is given in Table 1. For electrochemical studies, samples with the dimension of 10 mm × 10 mm × 0.1 mm were used. All chemicals were purchased from the Sigma-Aldrich and used as received. Metal samples were polished with abrasive sheets (120-1200 grade) and sonicated with acetone and washed with double distilled water. The chemical compositions of water which is used in system are characterized and tabulated in Table 2.

**Table 1:** Chemical composition of carbon steel specimen used in the present study.

Element	C	Mn	P	S	Al	Fe
Wt %	0.21	0.45	0.09	0.05	0.01	Balance

**Table 2:** Typical quality parameter data of the water used.

Parameters	Unit	(Min – Max)
Temperature	°C	23 – 31
Conductivity	µS/cm	265 - 317
Total dissolved Solids	mg/L	160 - 301
Total suspended Solids	mg/L	3 - 10
Dissolved oxygen	mg/L	3 – 4.7
pH	-	6.8 – 7.5
Total organic carbon	mg/L	5 – 86
Chloride	mg/L	40 - 70
Sulfate	mg/L	22 - 89
Calcium	mg/L	20 - 80
Magnesium	mg/L	5 - 60
Carbonate	mg/L	20 - 50
Bicarbonate	mg/L	20 - 60
Nitrate	µg/L	4.5 - 17
Nitrite	µg/L	0.004 – 0.45

### 2.2. ATR-FTIR spectroscopy

Attenuated Total Reflectance – Fourier Transform Infrared Spectroscopy (Perkin Elmer, USA) was used to find out the functional groups present in inhibitor.

### 2.3. Electrochemical measurements

Electrochemical studies were conducted using three electrode cell assembly systems at room temperature. Platinum and saturated calomel electrodes (SCE) were used as counter electrode and reference electrode respectively. Carbon steel sealed by epoxy resin with 1 cm<sup>2</sup> exposed surface areas was used as working

electrode. The experiments were performed using CH electrochemical work station. Impedance measurements were carried out in the frequency range of 100 kHz - 0.01 Hz with sinusoidal amplitude range of 0.01 V using AC signal at open circuit potential. Open circuit potential was recorded after half an hour immersion in electrolyte solution to get steady state open circuit potential followed by electrochemical impedance and potentiodynamic polarization experiments. All EIS data were simulated using ZsimpWin 3.22 software and comparison was obtained with fitted values.

Tafel polarization was carried out in 100 ml solution of electrolyte in the presence and absence of inhibitor from  $\pm 250$  mV with respect to OCP. The anodic and cathodic curves were extrapolated to corrosion potential to obtain corrosion current ( $i_{\text{corr}}$ ).

Electrochemical noises measurements were carried out in same CH electrochemical work station. A cell setup consisting of two identical mild steel as a working electrode ( $1\text{cm}^2$  surface areas) and calomel electrode used as a reference electrode. The working electrodes were prepared as mentioned for polarization and EIS studies. The electrochemical current and potential noises were measured between the two working with respect to the reference. All experiments were executed after half an hour immersion of electrode in the corrosive medium. 200 ml of test solution has been taken for each experiment.

#### 2.4. SEM/EDX

Surface characterization of the immersed metal in water medium in the absence and presence of optimum concentration of inhibitor was performed using SEM/EDX (Hitachi, Model S3400N, Japan).

#### 2.5. Atomic force microscope

Atomic force microscope (PARKSYSTEM) was used for surface roughness of the metal. Carbon steel coupons were exposed in the corrosive medium with and without the presence of optimum concentration of inhibitors for a day at 303 K. Metal coupons washed with water and acetone and used for further studies.

#### 2.6. QCA

The structural and electronic properties of -(4-chlorobenzoylmethyl) benzimidazoliumbromide molecule have been studied using first principle plane wave based periodic density functional theory (DFT) calculations, using Vienna Ab initio Simulation Package (VASP). In this calculation, the molecule is kept in large cubic unit cell with lattice constant of 25 Angstrom, to avoid the inter-molecular interactions. The electron-ions interactions are represented by projector augmented wave (PAW) pseudo-potential formalism and the electron-electron correlations are corrected by generalized gradient approximations (GGA). All the ions are relaxed to minimize the absolute forces less than 0.01 eV/Angstrom. The brillouin zone of the unit cell is sampled by Gamma point.

### 3. Results and discussion

#### 3.1. ATR-FTIR study

The ATR-FTIR spectrum of layer scratched from the metal surface without 3-(4-chlorobenzoylmethyl) benzimidazoliumbromide (a), pure inhibitor (b) and metal exposed in inhibitor mixed medium are shown in Fig. 1 (a-c), respectively. The broad peak at about  $3287\text{ cm}^{-1}$  implied the  $\text{OH}^-$  due to iron hydroxide. Its intensity become less in the presence of the optimum concentration of the inhibitor with the simultaneous appearance of peaks at about  $3388$  and  $3017\text{ cm}^{-1}$  due to the stretching frequencies of N-H and C-H stretching of hetero aromatic group. It is clear from the Fig (a) that the band at  $926\text{ cm}^{-1}$  referred to Fe-O-OH while, the Fe-O peaks confirmed by  $580\text{ cm}^{-1}$  frequency.

The peak at about  $744\text{ cm}^{-1}$  represents the C-H deformation of mono substituted benzene. C-N stretching of the benzimidazole appeared at  $1532\text{ cm}^{-1}$  where the peak was intense. The C=O stretching frequency in phenylacyl group of inhibitor appeared at  $1682\text{ cm}^{-1}$ . In addition, the bands obtained at  $820$ ,  $790$ ,  $502$  and  $1404\text{ cm}^{-1}$  were confirms the benzimidazole nature in the inhibitor. There is no change with respect to the intensity of oxygen in C=O both in the isolated condition and in the associated form with water medium. The desertion N-H peak in the spectrum (c) state that adsorption takes place by nitrogen and not by oxygen atom.

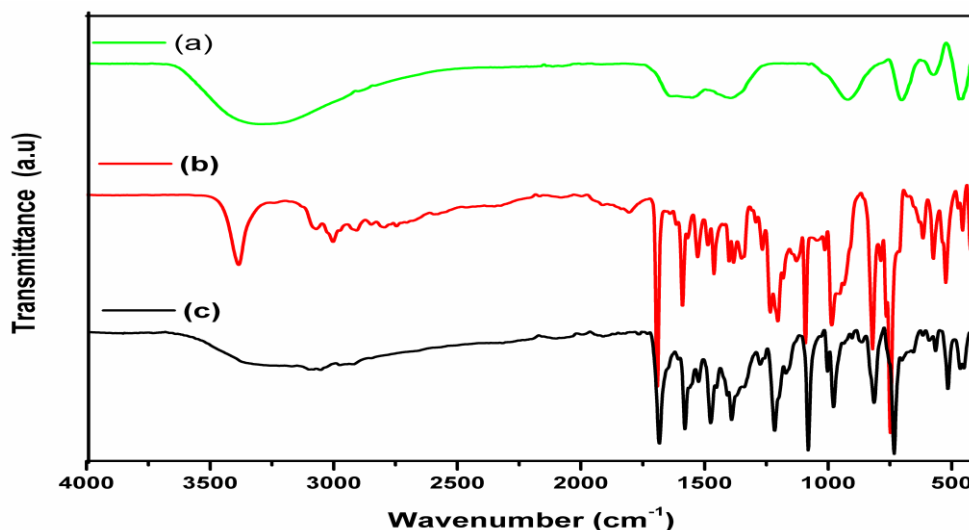


**Figure 1:** ATR-FTIR spectrum of a) Rust, b) inhibitor and c) adsorbed inhibitor on the surface.

### 3.2. Electrochemical impedance spectroscopy

Electrochemical impedance spectroscopy plays a vital role in investigate the protective layer formation on the metal surface. The impedance spectrum of carbon steel in water medium in the presence and absence of 3-(4-chlorobenzoylmethyl) benzimidazoliumbromide are shown in Fig. 2(a, b and c). The electrochemical impedance parameters such as charge transfer resistance ( $R_{ct}$ ), constant phase element (CPE) and solution resistance ( $R_s$ ) were calculated from Nyquist plot and were tabulated in Table 3. The general shape of the Nyquist plots remains same despite the addition of the inhibitor. All plots in the figure are depressed loops with single time constant. This can be attributed to the charge transfer process occurring between metal and electrolyte both in the presence and absence of 3-(4-chlorobenzoylmethyl) benzimidazoliumbromide in the water medium. The gradual increase of semicircle width (Fig. 2a) shows the adsorption of inhibitor on the metal surface as a function of  $R_{ct}$ . Obviously, it indicates the reduction in corrosion rate of the metal in the medium.

**Table 3:** The electrochemical impedance parameters of carbon steel in the presence of different concentration of 3-(4-chlorobenzoylmethyl) benzimidazoliumbromide.

Inhibitor (ppm)	$R_s$ ohm	CPE $Y_0(\mu F S^n / cm^2)$	$n$	$C_{dl}$ ( $\mu F/cm^2$ )	$R_{ct}$ ( $\Omega cm^2$ )	IE %
Blank	4.2	1739.0	0.5	132	85.0	-
100	1.3	495.6	0.7	93	240.5	64.6
200	1.6	340.9	0.7	52	399.9	78.7
300	2.1	138.2	0.8	38	777.4	89.0
400	1.8	111.7	0.8	26	557.7	84.7

The depressed semi circle in Nyquist plots indicates the metal roughness, distribution of active sites and adsorption of inhibitor [21, 22]. Constant phase element (CPE) is used as an alternate for the  $C_{dl}$  to get precise fitting [23]. The interaction of 3-(4-chlorobenzoylmethyl) benzimidazoliumbromide on the metal surface results in the formation of a passive layer. This passive layer behaves as a barrier for the charge transfers from metal to electrolyte leading to an increase in  $R_{ct}$  and decreases in  $C_{dl}$  values. From IR studies, it confirms that the passive layer adsorbed on metal surface. As the concentration of inhibitor increases, barrier thickness also increases at each concentration level. The contrary relation between  $R_{ct}$  and  $C_{dl}$  could attributed to decreasing values of local dielectric constant and/ or increase of double layer thickness of electrical double layer at the film/ metal interface [24, 25]. Inhibition efficiency can be calculated using the following equation mentioned below.

$$IE = \frac{R_{ct(inh)} - R_{ct}}{R_{ct(inh)}} \times 100 \quad (1)$$

$R_{ct(inh)}$  and  $R_{ct}$  are the charge transfer resistances in presence and absence of inhibitor, respectively. From Table 3, it can be observed that inhibition efficiency increases with increase in the inhibitor concentration. The maximum efficiency of 89% was obtained at 300 ppm. All the parameters viz, CPE and  $R_{ct}$  have been simulated mathematically using the equivalent circuit as represented in Fig. 3. The  $C_{dl}$  value is calculated by the given equation (2).

$$C_{dl} = Y_0 (\omega)^{n-1} \quad (2)$$

Where  $C_{dl}$  is the double layer capacitance,  $Y_0$  is the admittance of corrosive medium,  $\omega$  is the angular frequency ( $\omega = 2\pi f_{max}$ ) at which the imaginary part of impedance is maximum and  $f_{max}$  is frequency at maximum. However, displacement of water molecule by inhibitor on the metal surface results in the decrease in metal degradation and is reflected in the decrease in admittance from 1739 to 138  $\mu F S^{\beta}/cm^2$  as well as decrease in capacitance in the range from 132 to 26  $\mu F/cm^2$ . On the contrary,  $R_{ct}$  of the metal in water medium increases as the concentration of inhibitor increases, because of the adsorption of inhibitor on the active site as well as decrease in cathodic reaction.

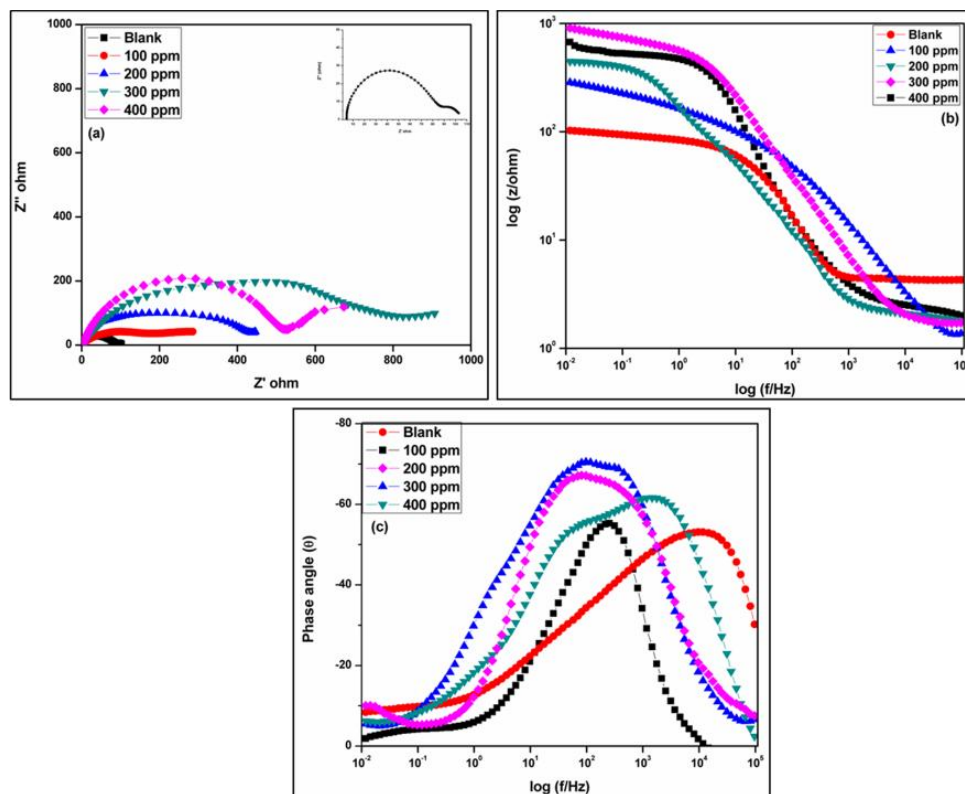


**Figure 2:** (a) Nyquist, (b) Bode impedance and (c) Bode phase angle plots for different concentrations of 3-(4-chlorobenzoylmethyl) benzimidazoliumbromide on carbon steel.

Bode impedance value increases gradually (Fig. 2b) as the inhibitor concentration increases (1 fold increment than that of blank). Graph represent well defined single time constant peak for both blank and different inhibitor concentration medium. This magnitude is merely consistent with Nyquist plots. The impedance value at lower frequency increased at each concentration level, which was the parameter to the corrosion protection by protective layer govern by adsorption of 3-(4-chlorobenzoylmethyl) benzimidazoliumbromide. It is notice that the maximum impedance value obtained at 300 ppm. Furthermore, the increased concentrations of inhibitor molecule favor the combat between the adsorbed inhibitor on the metal surface and free inhibitor in solution thereby resulting in the removal of the passivation. As a consequence, the charge transfer resistance decreased considerably.

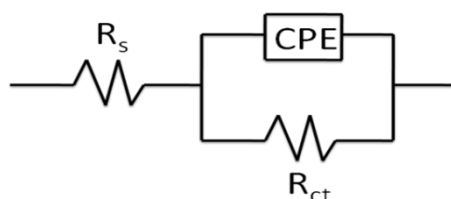


**Figure 3:** Equivalent circuit diagram.

The phase angle (Fig. 2c) of blank medium appears at about  $10^{-5} - 10^{-4}$  Hz as a single peak, it could be charge transfer process at metal/electrolyte. This peak has shifted to around  $10^{-3} - 10^{-2}$  Hz but the phase angle value retain as that of blank, is due to the passivation effect of coating formed by inhibitor and then each higher concentration level the phase value started to increase in the mid frequency. The lower phase angle implied about the surface roughness of metal. The shifting of phase from higher to lower range alongside of increases in phase angle were enlighten about the inhibitor adsorption process, forming passivation. The phase angle increases with increase in the concentration of inhibitor with a simultaneous shifting towards low frequency indicating strong coating effect of 3-(4-chlorobenzoylmethyl) benzimidazoliumbromide on the metal surface [26]. The highest phase angle value of  $-75^{\circ}$  occurred in the range of  $10^{-3} - 10^{-1}$  Hz. The phase angle has decreased after a while, in low frequency range. This behavior observed for all concentration curve of the metal is remains single time constant.

### 3.3. Potentiodynamic polarization studies

#### 3.3.1. Effect of inhibitor concentration

Fig. 4 shows the potentiodynamic polarization curves of carbon steel in water medium with various concentrations of 3-(4-chlorobenzoylmethyl) benzimidazoliumbromide at room temperature. Polarization parameters like corrosion potential ( $E_{corr}$ ), corrosion current ( $i_{corr}$ ), polarization resistance  $R_p$ , anodic Tafel slope constant ( $\beta_a$ ), cathodic Tafel slope constant ( $\beta_c$ ) and inhibition efficiency (IE) are shown in the Table 4. From the Table, it can be clearly seen that when inhibitor concentration increases corrosion current decreases. Inhibition efficiency of inhibitor in the medium has been calculated using the following equation (3) and it was observed that it increased with increasing inhibitor concentration.

$$IE = \frac{i_{corr} - i_{corr (inh)}}{i_{corr}} \times 100 \quad (3)$$

Where  $i_{corr}$  is the corrosion current in the absence of inhibitor and  $i_{corr (inh)}$  is the corrosion current in the presence of inhibitor.

**Table 4:** Polarization parameters of carbon steel at various concentrations of 3-(4-chlorobenzoylmethyl) benzimidazoliumbromide at room temperature.

Inhibitor (ppm)	$-E_{corr}$ (V)	$\beta_a$ (mV/dec)	$-\beta_c$ (mV/dec)	$i_{corr}$ (A/cm <sup>2</sup> )	$R_p$ (Ω/cm <sup>2</sup> )	IE %
Blank	0.523	5.9	7.6	$5.254 \times 10^{-4}$	61	-
100	0.515	11.9	10.5	$1.088 \times 10^{-4}$	178	79.2
200	0.560	6.0	6.1	$9.20 \times 10^{-5}$	389	82.4
300	0.516	10.0	5.2	$2.17 \times 10^{-5}$	899	95.8
400	0.540	11.4	9.1	$2.84 \times 10^{-5}$	740	94.5

The cathodic or anodic behavior of the inhibitor can be determined by corrosion potential shift with respect to the blank. A shift was more than -85 mV indicates that it is a cathodic inhibitor and a shift of the same magnitude towards the opposite side ie, +85 mV designates anodic inhibitor.  $E_{corr}$  values of different inhibitor

concentrations reveal that there is no significant change in them. The maximum displacement was 37 mV hence it is a mixed type inhibitor [27].

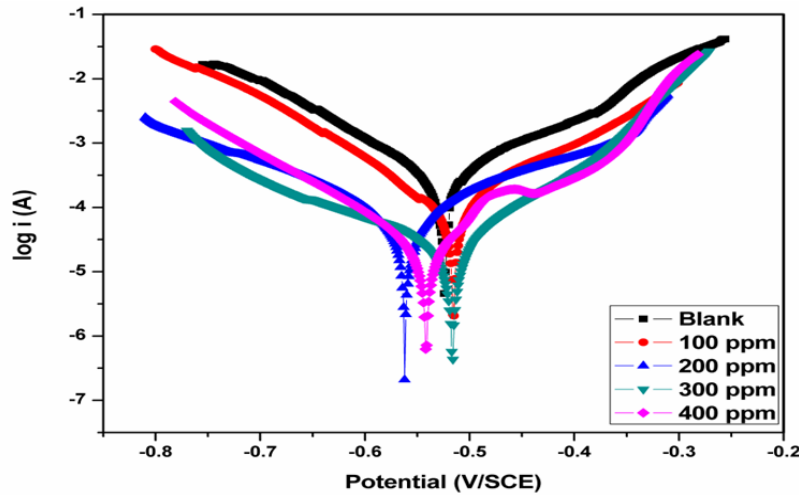


**Figure 4:** Potentiodynamic polarization curves for different concentrations of 3-(4-chlorobenzoylmethyl) benzimidazoliumbromide on carbon steel.

The addition of inhibitor hasn't changed the mechanism of metal dissolution and obviously it was reflected in anodic and cathodic Tafel slope constants, which almost remain constant. Table 4 shows the gradual increase of  $R_p$  values with increases of inhibitor concentration, due to blockage of active areas by the inhibitor on the metal surface indicating formation of passive film on the metal surface [28] thus arresting the corrosion of metal. As the polarization resistance increases, the corrosion rate diminishes. The maximum inhibition efficiency of 94% was observed which data is in close agreement with EIS.

### 3.3.2 Effect of pH in medium

The influences of pH in the range of 1-7 on the corrosion rate and inhibition efficiency are displayed in Fig. 5.

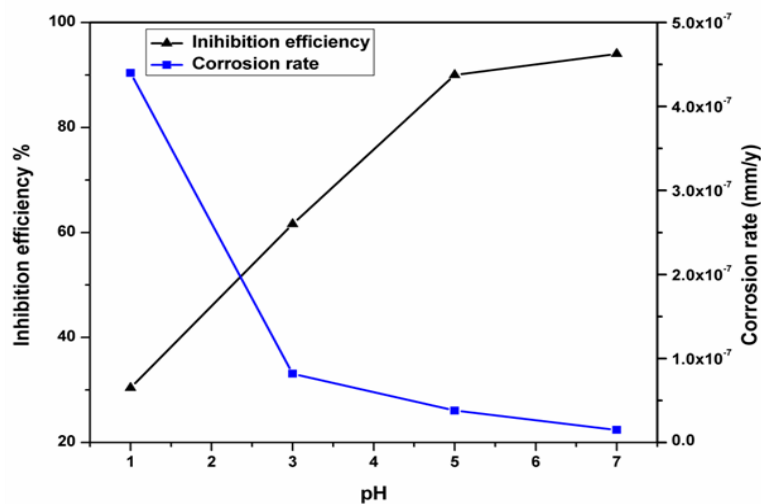


**Figure 5:** Effect of pH on corrosion rate and inhibition efficiency in water medium.

The graph reveals that the inhibition efficiency increases from 30 to 94% with pH increases from 1 to 7 which are attributed to the passive productive film layer of inhibitor on the metal substrate. An optimum concentration of 300 ppm was used for all experiments at room temperature. The increase of inhibition efficiency of 3-(4-chlorobenzoylmethyl) benzimidazoliumbromide reflects in a converse effect on corrosion rate obtained at pH 1. The reason for the decrease in inhibition efficiency with decrease in pH from 7 to 1 is because of more  $H^+$  concentration. Due to high concentration of  $H^+$ , the medium become more acidic which lead to high corrosion

rate. In neutral condition the probability of adsorption of 3-(4-chlorobenzoylmethyl) benzimidazoliumbromide on the metal surface is enhanced compared to other lower pH values. Hence, the inhibition efficiency increases with low corrosion rate.

### 3.3.3. Effect of temperature

The effect of temperature on the inhibition efficiency of carbon steel in water medium in the absence and presence of optimum concentration of 3-(4-chlorobenzoylmethyl) benzimidazoliumbromide are shown in Fig. 6. The inhibition efficiency decreases with increase in the solution temperature from 303 to 333 K. Accordingly, increasing the temperature increases the corrosion rate from 0.46 to  $3.7 \times 10^{-7}$  mm/y. The reason is that increases in temperature results in desorption of passive layer from carbon steel surface [29, 30]. At high temperature the equilibrium between adsorption and desorption relocate to later, leads to high corrosion rate [31]. Increase in temperature is accompanied by increase in cathodic as well as anodic current density and results in increased corrosion rate.

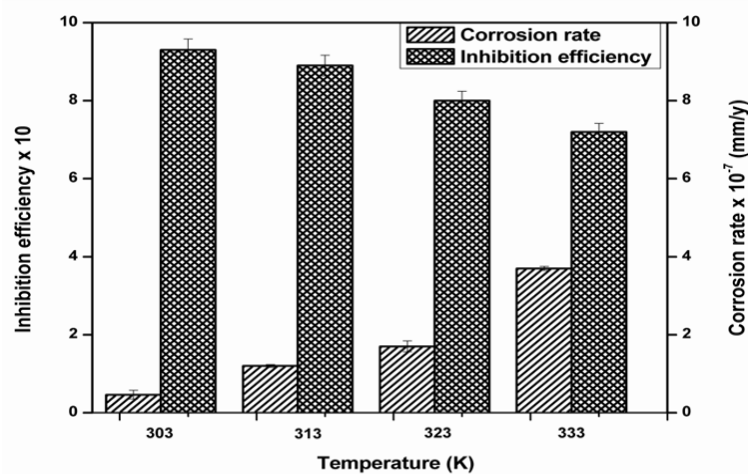


**Figure 6:** Temperature effect on inhibition efficiency and corrosion rate of carbon steel at optimum concentration 3-(4-chlorobenzoylmethyl) benzimidazoliumbromide.

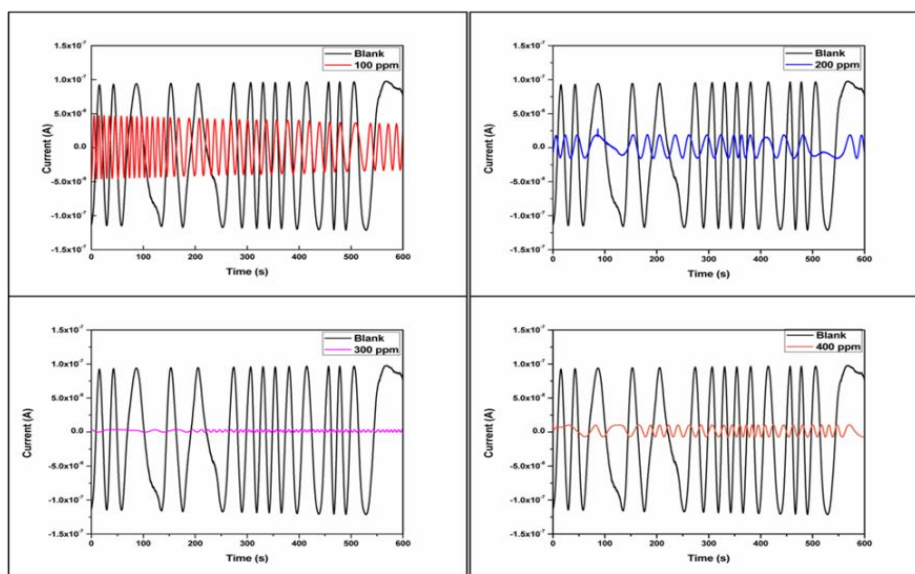
### 3.4. Electrochemical noise analysis

Fig. 7 illustrates the electrochemical current noise for the carbon steel in water medium without inhibitor and containing various concentrations of 3-(4-chlorobenzoylmethyl) benzimidazoliumbromide. It is shown that the amplitude of current noise of the blank is higher than that of the sample engrossed in inhibited medium [32]. In each concentration level the amplitude of current dwindles gradually, it is totally attributed to the passivation formed by the inhibitor.

The extreme decrease of current noise obtained at 300 ppm of 3-(4-chlorobenzoylmethyl) benzimidazoliumbromide. The noise amplitude gets increased at 400 ppm. This is because of commencing of delaminating of adsorbed film from the metal surface. Hence the noise produced with high amplitude so that the current deviation also increased. The electrochemical noise parameter viz, potential deviation ( $\sigma E$ ), current deviation ( $\sigma I$ ) and noise resistance ( $R_n$ ) are determined and listed in Table 5. The maximum inhibition efficiency attained at 300 ppm of 3-(4-chlorobenzoylmethyl) benzimidazoliumbromide. The maximum IE trend attained at 300 ppm from polarization and impedance was merely good in agreement with ENA. The inhibition efficiency can be calculated using the following equation (4).

$$IE = \frac{R_n - R_n^0}{R_n} \times 100 \quad (4)$$

$R_n$  and  $R_n^0$  be the noise resistance of the sample exposed to the inhibitor and blank medium respectively.



**Figure 7:** Electrochemical current noise obtained from carbon steel in the absence and presence of various concentration of 3-(4-chlorobenzoylmethyl) benzimidazoliumbromide.

**Table 5:** Electrochemical noise parameter obtained from carbon steel in the presence and absence of 3-(4-chlorobenzoylmethyl) benzimidazoliumbromide.

Inhibitor (ppm)	$\sigma I$ ( $\times 10^{-8}$ A)	$\sigma E$ ( $\times 10^{-3}$ V)	$R_n$ ( $\times 10^4 \Omega \text{ cm}^2$ )	IE (%)
Blank	7.616	3.887	5.104	-
100	2.859	2.182	7.632	33.1
200	1.167	1.250	10.71	52.3
300	0.131	15.11	1152	99.5
400	0.631	0.3739	5.923	13.8

### 3.5. Adsorption isotherm and thermodynamic properties

Adsorption of the inhibitors on the metal surface is the essential step in tracing the inhibition process [33]. The inhibitor could relate with the metal either by physical adsorption or chemical adsorption. Interaction of the inhibitor on metal solution interface proceeds through any of the following ways (a) the interaction of unshared pair of electrons in the inhibitor molecule with the metal surface, (b) the interaction of  $\pi$ - electrons of the inhibitor with the metal, (c) the electrostatic attraction between the charged inhibitor molecule and the charged metal or (d) the combination of all the three [34]. The inhibitive property of inhibitor mainly depends on the availability of  $\pi e^-$  in its structure and large molecular size which insures greater coverage of metallic surface. The adsorption process of the inhibitors is greatly influenced by structure, charge distribution and nature of the metal [35]. The degree of the surface coverage of the metal can be calculated using the following formula. Langmuir adsorption is obeyed by increasing of surface coverage due to enhanced inhibitor concentration and obtains the maximum coverage.

$$\theta = \frac{I_{\text{corr}} - I_{\text{corr(inh)}}}{I_{\text{corr}}} \quad (5)$$

Where,  $\theta$  is the surface coverage area,  $I_{\text{corr}}$  and  $I_{\text{corr(inh)}}$  are corrosion currents of blank and inhibitor medium. Many attempts were made to fit the  $\theta$  values to various isotherms including Langmuir, Temkin, Freundlich and Frumkin. The best fit is obtained with the Langmuir isotherm [36]. In the scrutinizing of inhibition mechanism of an inhibitor, thermodynamic properties are very important. The adsorption equilibrium relation is given in the following equation.

$$K_{ads} = \frac{\theta}{(1 - \theta)C} \quad (6)$$

Where,  $K_{ads}$  is the adsorption equilibrium constant,  $\theta$  is the surface coverage and  $C$  is the concentration of the inhibitor. The plot of  $C/\theta$  vs  $C$  gives a straight line as shown in Fig. 8. The slope of the graph was closed to unity, confirming the Langmuir adsorption isotherm. Larger the value of  $K_{ads}$ , better is the efficiency of adsorption of inhibitor.

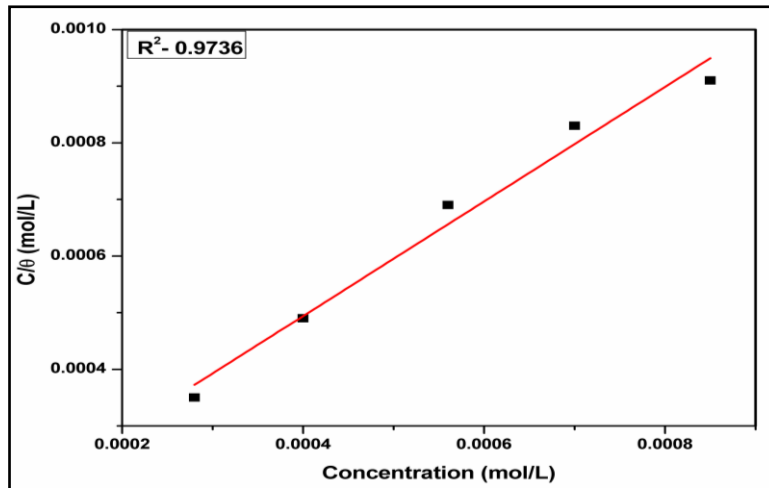


**Figure 8:** Langmuir adsorption isotherms of 3-(4-chlorobenzoylmethyl) benzimidazoliumbromide on carbon steel at different concentration in water medium.

Thermodynamic properties of the inhibitor are necessary to relate inhibition mechanism on carbon steel with the adsorption of inhibitor. Free energy of adsorption ( $\Delta G_{ads}$ ) of the inhibitor was calculated using the following relation (7):

$$\Delta G_{ads} = -RT \ln(55.5 K_{ads}) \quad (7)$$

The negative value of  $\Delta G$  indicates the stability of the protective film on the metal substrate and spontaneity of the adsorption process. From Table 6, it is clearly seen that free energy of adsorption value becomes less negative with the decrease in  $K_{ads}$  which indicates desorption of inhibitor as function of increasing temperature. If the  $\Delta G > -40$  kJ/mol, the adsorption of the inhibitor is said to be chemisorption or  $\Delta G < -20$  kJ/mol then it will be physisorption [37]. The calculated  $\Delta G$  value for the inhibitor is around -34 kJ/mol and hence the adsorption of inhibitor in its medium is both by physical and chemical adsorption. The increase of  $\Delta G$  indicates exothermic process of 3-(4-chlorobenzoylmethyl) benzimidazoliumbromide adsorption on the metal/electrolyte interface [38].

**Table 6:** Equilibrium constant and free energy of adsorption of optimum concentration of 3-(4-chlorobenzoylmethyl) benzimidazoliumbromide at different temperature.

Inhibitor	Temperature K	$K_{ads}$ mol <sup>-1</sup>	$-\Delta G_{ads}$ k J mol <sup>-1</sup>
3-(4-chlorobenzoylmethyl) benzimidazoliumbromide	303	18301	34.8
	313	10124	34.4
	323	4789	33.5
	333	3107	33.3

$$\log(\text{rate}) = \frac{-E_a}{2.303 RT} + A \quad (8)$$

Where,  $E_a$  is the activation energy,  $R$  is the gas constant,  $T$  is the absolute temperature and  $A$  is Arrhenius pre-exponential constant. The Arrhenius plots of  $\ln CR$  vs  $1/T$  for the blank and 3-(4-chlorobenzoylmethyl) benzimidazoliumbromide are shown in Fig. 9. From the slope of the graph activation energy ( $E_a$ ) can be

calculated. The activation energy for the inhibitor medium is higher than the blank by an amount of 71.2 kJ/mol. The increase in  $E_a$  is due to the passive film layer which retards the metal dissolution reaction thereby favoring the lesser corrosion rate [39]. The electrostatic adsorption behavior was strongly confirmed by decreasing of inhibition efficiency and increasing of  $E_a$  with temperature of the medium and concentration of inhibitor, respectively.

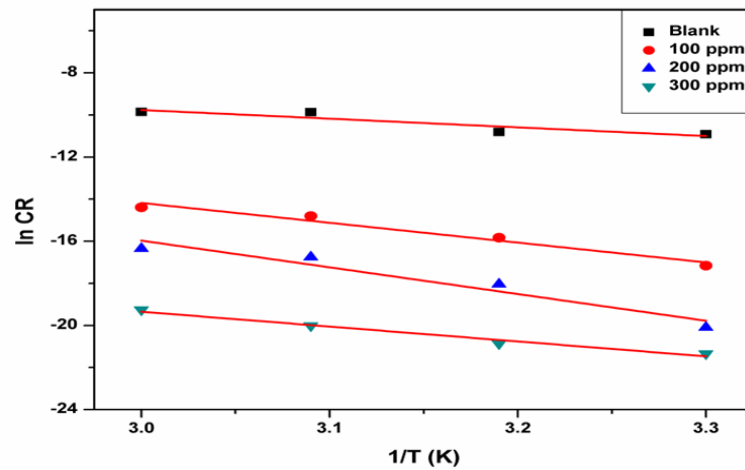


**Figure 9:** Arrhenius plots for carbon steel in the absence and presence of 3-(4-chlorobenzoylmethyl) benzimidazoliumbromide.

Arrhenius transition state equation is used to find out the entropy and enthalpy of the inhibitor adsorption process as given below equation (9).

$$CR = \frac{RT}{Nh} \exp\left(\frac{\Delta S}{R}\right) \exp\left(-\frac{\Delta H}{RT}\right) \quad (9)$$

Where  $N$  is the Avogadro number,  $h$  is the Planck's constant,  $\Delta S$  is the entropy of activation and  $\Delta H$  is the enthalpy of activation and these parameters were calculated by plotting between  $\ln(CR/T)$  against  $1/T$  ( as shown Fig. 10).

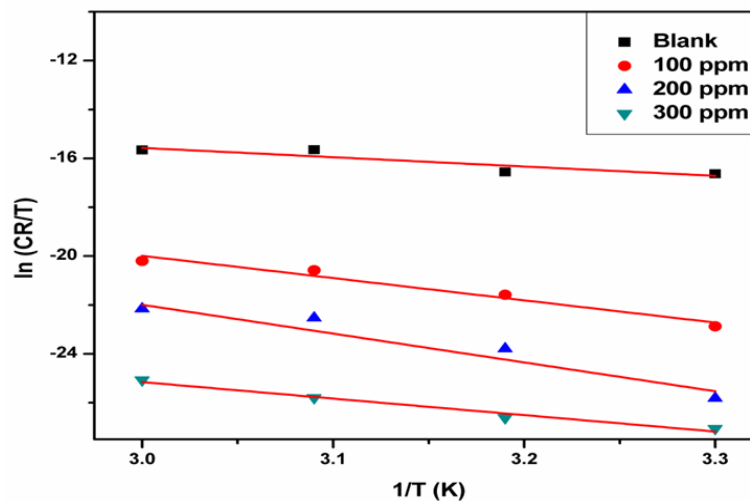


**Figure 10:** Transition state plot of carbon steel in the absence and presence of 3-(4-chlorobenzoylmethyl) benzimidazoliumbromide.

The graph gives a straight line with slope value of  $-\Delta H/R$  and intercept value of  $\ln(R/Nh)+(\Delta S/R)$ , tabulated in Table 7. In each high concentration level of the inhibitor  $\Delta H$  and  $E_a$  attained high values. This indicates that more energy barrier has been utilized to obtain activated state. In the presence of 3-(4-chlorobenzoylmethyl) benzimidazoliumbromide,  $\Delta S$  acquired large negative value which implied that the rate determining step favors the activated complex formation by the association process [40, 41].

**Table 7:** Thermodynamic parameters for carbon steel obtained from polarization studies.

Inhibitor	Concentration ppm	Ea k J mol <sup>-1</sup>	-ΔH <sub>ads</sub> k J mol <sup>-1</sup>	-ΔS <sub>ads</sub> J mol <sup>-1</sup> K <sup>-1</sup>
3-(4-chlorobenzoylmethyl) benzimidazoliumbromide	blank	34.2	31.6	51.7
	100	62.5	56.1	43.7
	200	78.3	75.7	38.3
	300	105.4	98.8	31.4

### 3.6. SEM/EDX

The SEM images of the carbon steel are shown in Fig. 11(a, c and e) the corresponding EDX are depicted in (b, d and f). The bare metal substrate exhibit grooves on its surface due to grinding. After exposure of metal in blank medium, the metal surface is dissolved at the metal/solution interface and forms pyramidal shaped corroded particles on the whole surfaces uniformly and it was confirmed by EDX, the oxygen peak due to the hydroxide of iron with the medium [42]. The metal immersed in inhibitor medium was highly covered with the needle shaped cluster of 3-(4-chlorobenzoylmethyl) benzimidazoliumbromide on entire surface. In addition to that, the adsorption of the inhibitor was confirmed by the presence of nitrogen and oxygen peaks in the EDX (f) spectrum. In the presence of optimized concentration of inhibitor, corrosion rate of carbon steel was reduced and hence there is little corrosion product on the surface. The amount of corrosion products formed with inhibitor medium is lesser than with the blank medium which could be attributed to the inhibitive action of inhibitor in the medium.

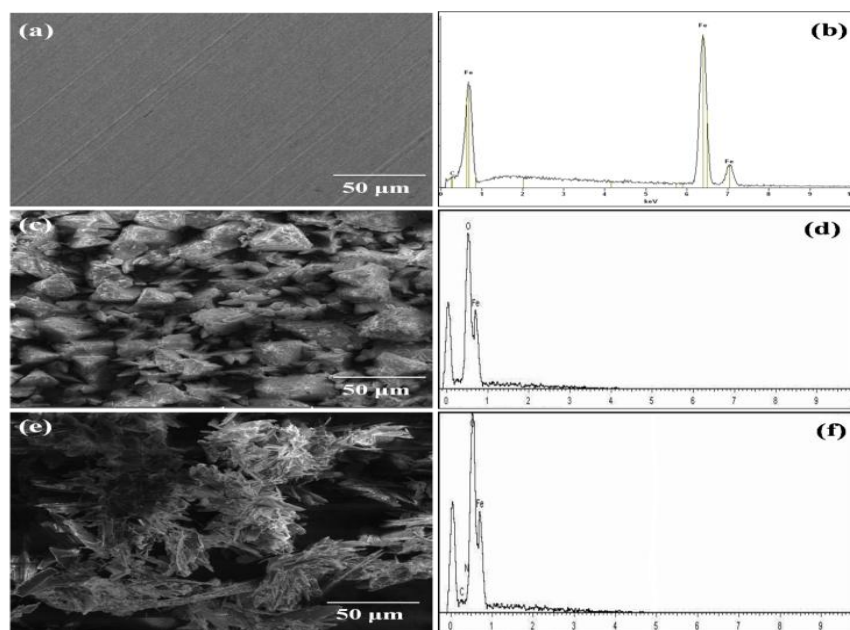


**Figure 11:** (a) Bare metal (b) EDX of bare metal (c) Metal immersed in blank (d) EDX of metal immersed in blank (e) Metal immersed in inhibitor medium for (f) EDX of metal immersed in inhibitor medium for 24 h.

### 3.7. Atomic force microscope

The atomic force microscope provides information of microstructure surface roughness of mild steel in the presence and absence inhibitor medium. Fig. 12 shows the 3 D and 2 D image of the metal. Fig. 12 (a) shows 3 D image of the bare metal, its average roughness value of the polished sample was determined to be 11 nm. When it is subjected to contact with electrolyte medium, conversion of metal to ion process initiated. As the phenomenon carried out further the surface became non-uniform with crest and trough. Accordingly, the metal surface roughness which is exposed in blank medium is higher, due to the attack of the corrosive ion on the surface. The surface roughness of polished mild steel will be lower than that of the exposed in aggressive medium and it has the value of 80 nm as shown in Fig. 12 (c). The illustration of Fig. 12 (e) has the lowest

roughness value of 49 nm due the passive layer of inhibitor formed on the surface which obstructs the further ingress of corrosive ion. This 3-(4-chlorobenzoylmethyl) benzimidazoliumbromide film performs as geometric blocking area which will safeguard the underlying metal [43]. Hence, it is significantly reduced to 49 nm in the presence optimum concentration of inhibitors.

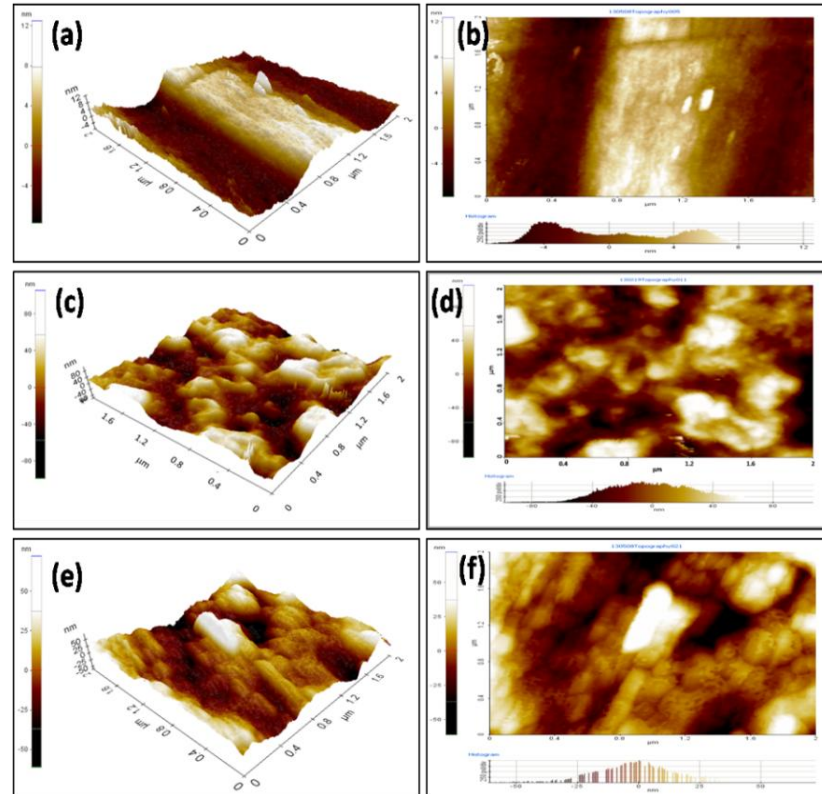


**Figure 12:** (a) 3 D (b) 2 D image of bare metal, (c) 3 D (d) 2 D image of metal exposed in blank medium and (e) 3 D (f) 2 D image of metal exposed in inhibitor medium for 24 h.

### 3.8. Quantum chemical analysis (QCA)

Quantum chemical analysis is used to investigate the adsorption process of inhibitor and it is a proven method to determine the electronic structure and reactivity. Quantum chemical analysis is important in the study of electronic interaction between metal and inhibitors. Hence, it has become important method in corrosion inhibition studies. The fully optimized geometry, Mulliken charge distribution, highest occupied molecular orbital and lowest unoccupied molecular orbital were shown in Fig. 13(a-d). The quantum chemical parameters like highest occupied molecular orbital (HOMO), lowest unoccupied molecular orbital (LUMO), Separation energy  $\Delta E$  ( $E_{LUMO} - E_{HOMO}$ ), electro negativity ( $\chi$ ), hardness ( $\eta$ ), softness ( $\sigma$ ), ionization potential (IP) and electron affinity (EA) are calculated using the following relations. The values are shown in the Table 8.

$$\Delta N = \frac{\chi_{Fe} - \chi_{inh}}{2(\eta_{Fe} + \eta_{inh})} \quad (10)$$

$$\chi = \frac{IP + EA}{2} \quad (11)$$

$$\eta = \frac{IP - EA}{2} \quad (12)$$

$$\sigma = \frac{1}{\eta} \quad (13)$$

$$IP = -HOMO \quad (14)$$

$$EA = -LUMO \quad (15)$$

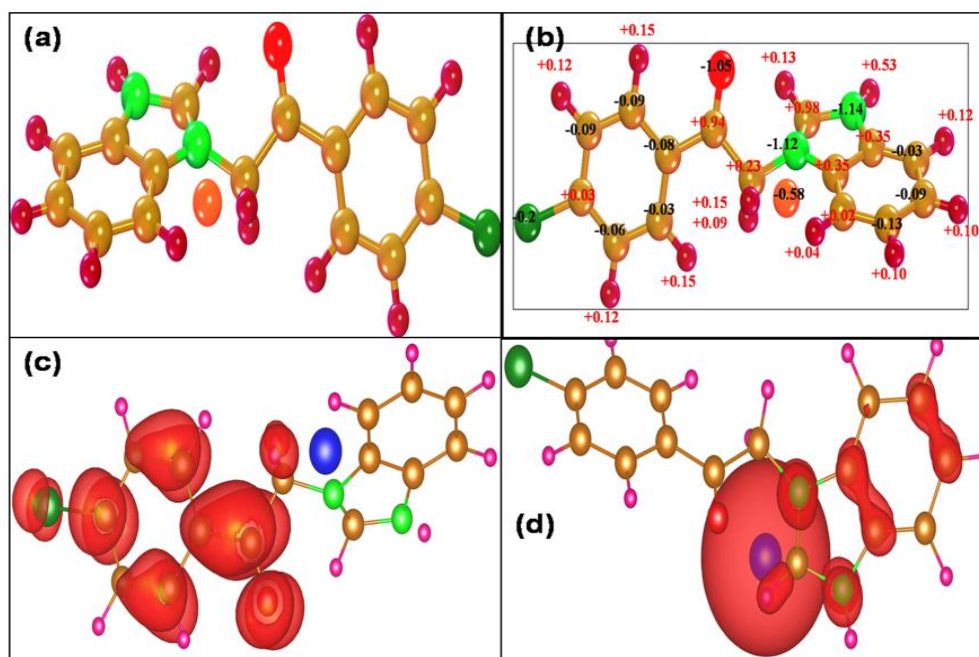


**Figure 13:** (a) Optimized geometry, (b) Mulliken charge distribution, (c) HOMO and (d) LUMO of 3-(4-chlorobenzoylmethyl) benzimidazoliumbromide.

Highest energy of  $E_{\text{HOMO}}$  of the inhibitor can be able to offer electron to the empty orbital or lowest energy orbital of metal [44]. Similarly, low energy of  $E_{\text{LUMO}}$  indicates withdrawing tendency of electron from the environment. A compound to be effective in inhibition efficiency it should possess high value of  $E_{\text{HOMO}}$  and low value of  $E_{\text{LUMO}}$ . The separation energy between the  $E_{\text{HOMO}}$  and  $E_{\text{LUMO}}$  reveals the stability of the molecule. Table 8 shows 3-(4-chlorobenzoylmethyl) benzimidazoliumbromide has high  $\Delta E$  value which implied that high energy requires to removing an electron from its outer most orbital and this said to be hardness of the molecule. It is known that the molecule is so hard, electrons will not be transferred. Low  $\Delta E$  value of the compound possesses highest inhibition efficiency [45].

**Table 8:** Quantum chemical parameters of 3-(4-chlorobenzoylmethyl) benzimidazoliumbromide.

HOMO (eV)	LUMO (eV)	$\Delta E$ (eV)	IP (eV)	EA (eV)	$\chi$ (eV)	$\eta$ (eV)	$\sigma$	$\Delta N$	Binding energy k cal/mol
-5.0555	-3.1240	1.9315	5.0555	3.1240	4.0897	0.9657	1.0355	1.5	4483

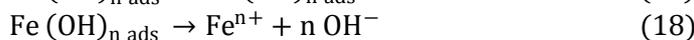
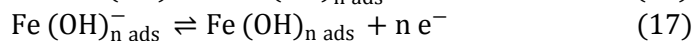
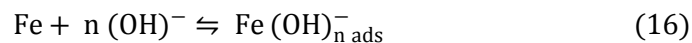
An excellent inhibitor compound not only donates but also accepts the electrons from the metal to its anti bonding orbital to form feedback bond [46]. Higher the binding will favor the adsorption of the inhibitor molecule to form the passive film on the metal surface [47]. The binding energy of the inhibitor is 4483 k cal/mol, indicates that the binding of inhibitor on the metal surface quite easier. Fig. 14(c) explores the higher electron density distribution on phenyl ring of the compounds. However it is whirling around only in benzimidazolium ring at LUMO Fig. 14(d). Highest value of  $\Delta E$  and lowest value  $\sigma$  reflects the inability of 3-(4-chlorobenzoylmethyl) benzimidazoliumbromide to part with its electron in the interaction between inhibitor molecule and metal surface for chemisorptions. Lesser value of  $\Delta N$  will facilitate the electron donating ability to the metal surface and hence inhibitor would have better electron offering tendency [48]. When inhibitor in the medium is in contact with metal, the flow of electrons proceed from lower electro negativity species to higher (i.e from inhibitor to Fe) till the balance between the chemical potentials is attained [49]. The literature revealed that the inhibition efficiency offered by 3-(4-chlorobenzoylmethyl) benzimidazoliumbromide was better than other azole based and its derivatives. [50-55]. The higher efficiency of 3-(4-chlorobenzoylmethyl)

benzimidazoliumbromide is attributed to the less  $\Delta E$  value between the HOMO and LUMO which facilitates easy electron transfer to metal surface. The above parameters calculated from quantum chemical study supports the protective nature of the passive layer of the inhibitor through its donating ability of electron thereby proving its better inhibition efficiency.

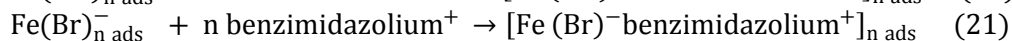
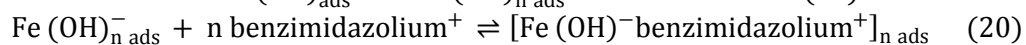
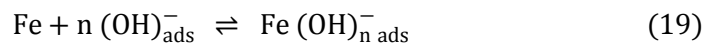
### 3.9. Surface adsorption mechanism of 3-(4-chlorobenzoylmethyl) benzimidazoliumbromide.

Adsorption is a surface phenomenon in which the molecules of gas or liquid or dissolved substances present in the medium are adhered on the surface of the metal substrate [7]. Carbon steel is initially oxidized to  $Fe^{2+}$  at anodic site. However, in the presence of  $OH^-$  and dissolved oxygen, the metal dissolution increases as per the following equations [56].

At anodic site:



More negative charge has been created on the metal surface by the adsorption of  $OH^-$  ion from the solution attracts positive ions present in the electrolyte medium. In inhibitor medium, the cationic part of 3-(4-chlorobenzoylmethyl) benzimidazolium bromide viz. benzimidazolium $^+$  is attracted by the negative charge on the substrate and is eventually followed by attraction of  $Br^-$  or  $OH^-$  ions by physical adsorption. In other words,  $Br^-$  in the 3-(4-chlorobenzoylmethyl) benzimidazoliumbromide integrates the positive metal surface with cationic part benzimidazolium $^+$  [57]. Hence the adsorption becomes stabilized by physical adsorption and results in higher surface coverage area and leads to least metal dissolution when it undergoes the following equations.



The adsorption of inhibitor will repel the already adsorbed water molecule and reduce further  $Fe (OH)_n$  production.

At cathodic site

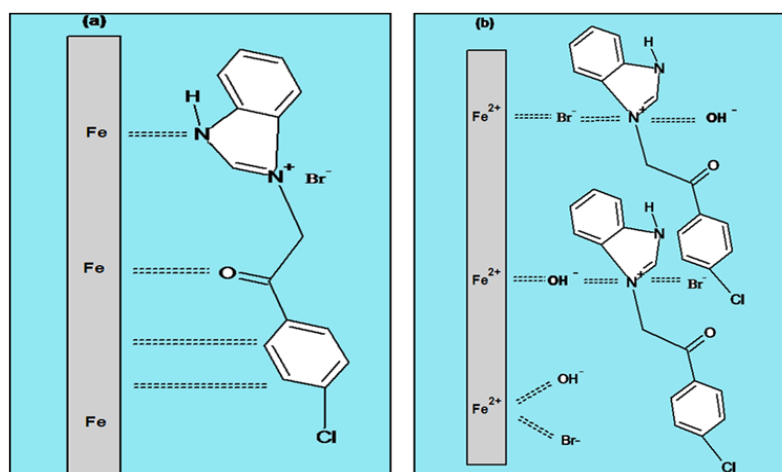
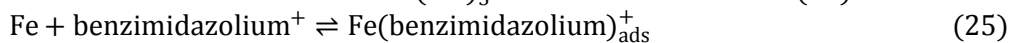
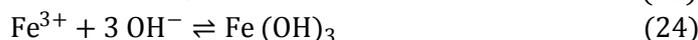


**Figure 14:** Pictorial representation of plausible adsorption mechanism a) chemisorption and b) physisorption of 3-(4-chlorobenzoylmethyl) benzimidazoliumbromide on carbon steel.

The hydroxyl ion is formed due to reduction reaction with water molecule. The corrosive product of iron hydroxide is formed as net electrochemical reaction. On the other hand,  $Fe^{2+}$  is oxidized to  $Fe^{3+}$  in the presence

of O<sub>2</sub> and further it generates out the iron (III) hydroxide followed by the passive film layer formation as per the equations shown below.



Adsorption of the inhibitor molecule can take place via three possibilities which could be anodic, cathodic and/or mixed inhibition mechanism. The adsorption can be extended by the following properties like nature and surface of the metal, chemical structure, mode of adsorption of inhibitor and corrosiveness of the medium. Finally, these are the outcome of adsorption or complex formation of inhibitor molecule with ion at the metal surface. Thermodynamic property reveals that the adsorption mechanism is totally attributed to both chemisorption (mono layer of active species) and physisorptions (multi layer of active species). The least value of  $\Delta E$  implies the e<sup>-</sup> donating nature of 3-(4-chlorobenzoylmethyl) benzimidazoliumbromide. The chemisorption takes place via the transfer of aromatic benzene  $\pi$  electron to the empty d- orbital ( $p\pi-d\pi$  bond formation) [58] or by the non bonding electron on the nitrogen and oxygen in its structure. In view of these evidences the possible mechanisms of adsorption are shown in Fig. 15.

## Conclusions

1. 3-(4-chlorobenzoylmethyl) benzimidazoliumbromide was found to be good corrosion inhibitor for carbon steel at 300 ppm with inhibition efficiency of 94 % in water medium.
2. The potentiodynamic polarization curve suggested that the 3-(4-chlorobenzoylmethyl) benzimidazoliumbromide was acted as mixed inhibitor.
3. EIS and ENA results were revealed that the optimum concentration of inhibitor significantly increased the corrosion resistance by forming barrier effect and noise resistance. The inhibition efficiency values of EIS and polarization studies more or less resembles with ENA data.
4. The adsorption of 3-(4-chlorobenzoylmethyl) benzimidazoliumbromide on carbon steel obeys Langmuir isotherm and inhibition efficiency increased with increasing inhibitor concentration and decreased with temperature. The spontaneous adsorption of 3-(4-chlorobenzoylmethyl) benzimidazoliumbromide on the metal surface was determined by thermodynamic properties
5. The reports of surface topology and elemental analysis of the metal before and after addition of inhibitor were described by SEM and EDX. Surface roughness decreased by injection of 3-(4-chlorobenzoylmethyl) benzimidazoliumbromide in medium.
6. The proper adsorption mechanism and electronic properties were examined via, HOMO and LUMO energy level of 3-(4-chlorobenzoylmethyl) benzimidazoliumbromide.

**Acknowledgement**-Authors gratefully acknowledge the Atomic Energy Regulatory Board (AERB: Project No. 48/01/2012/68) for the financial support to carry out this work. The instrument facilities provided by DST-FIST and UGC-DRS are gratefully acknowledged. Authors are very thankful to Dr. P. Murugan, Central Electrochemical Research Institute, Karaikudi for the characterization of quantum chemical analysis. Conflict of Interest: all the authors of this manuscript have no conflict of interest.

## References

1. Salasi M. Shahrabi T., Roayaei E., Aliofkhazraei M., *Mater. Chem. Phys.* 104 (2007) 183.
2. Badiae A.M., Mohana K.N., *Corros. Sci.* 51 (2009) 2231.
3. Dkhireche N., Dahami A., Rochdi A., Hmimou J., Tour R., Ebn Touhami M., El Bakri M., El Hallaoui A., Anouar A., Takenouti H., *J. Ind. Eng. Chem.* 19 (2003) 1996.

4. Tourir R., Dkhireche N., Ebn Touhami M., Lakhrissi M., Lakhrissi B., Sfaira M., *Desalination* 249 (2009) 922.
5. Agarwal P., Landolt D., *Corros. Sci.* 40 (1998) 673.
6. Xu Y., Zhang B., Zhao L., Cui Y., *Desalination*, 311 (2013) 156.
7. Mohana K.N., Badiea A.M., *Corros. Sci.* 50 (2008) 2939.
8. Tourir R., Dkhireche N., Touhami M.E., Bakri M.E., Rochdi A.H., Belakhmima R.A., *J. Saud. Chem. Soc.* DOI:10.1016/j.jscs.2011.10.020.
9. Abd El Khalek D.E., Abd El Nabey B.A., *Desalination* 311 (2013) 227.
10. Hams El Din S A.M., Wang L., *Desalination*. 107 (1996) 29.
11. A.E. Al Rawajfeh, E.M. Al Shamaileh, *Desalination*. 206 (2007) 169.
12. Tuken T., Demir F., Kicir N., Sigircik G., Erbil M., *Corros. Sci.* 59 (2012) 110.
13. Trombetta F., Souza R.F., Souza M.O., Borges C.B., Panno N.F., Martini E.M.A., *Corros. Sci.* 53 (2011) 51-58.
14. Murulana L.C., Singh A.K., Shukla S.K., Kabanda M.M., Ebenso E.E., *Ind. Eng. Chem. Res.* 51 (2012) 13282.
15. Bo Z.Q., Xin H.Y., *Acta Phys.Chim. Sin.* 27 (2011) 655.
16. Likhanova N.V., Xomet O.O., Lucero D.G., Domínguez aguilar M.A., Nava N., Luna M.C., Mendoza M.C., *Int. J. Electrochem. Sci.* 6 (2011) 4514.
17. Sorkhabi H.A., Eshaghi M., *Mater. Chem. Phy.* 114 (2009) 267.
18. Saleh M.M., *Mater. Chem. Phys.* 98 (2006) 83.
19. Khamis A., Saleh M.M., Awad M.I., *Corros., Sci.* 66 (2013) 343.
20. Likhanova N.V., Dominguez Aguilar M.A., Xomed O.O., Entzana N.N., Arce E., Dornates H., *Corros. Sci.* 52 (2010) 2088.
21. Sanatkumar B.S., Nayak J., Nityananda Shetty A., *Int. J. Hydrogen Energy.* 37 (2012) 9431.
22. Musa A.Y., Jalgham R.T.T., Mohamad A.B., *Corros. Sci.* 56 (2012) 176.
23. Kumar Singh A., Ebenso E.E., *Int. J. Electrochem. Sci.* 7 (2012) 2349.
24. Ibrahim T., Alayan H., Mowaqet Y.A., *Prog. Org. Coat.* 75 (2012) 456.
25. Golestani Gh., Shahidi M., Ghazanfari D., *Appl. Surf. Sci.* <http://dx.doi.org/10.1016/j.apsusc.2014.04.172>
26. Zhou X., Yang H., Wang F., *Electrochim. Acta.* 56 (2011) 4268.
27. Ahamad I., Prasad R., Quraishi M.A., *Corros. Sci.* 52 (2010) 3033.
28. Solmaz R., Kardas G., Culhab M., Yazıcı B., Erbil M., *Electrochim. Acta.* 53 (2008) 5941.
29. Zhang Q.B., Hua Y.X., *Electrochim. Acta.* 54 (2009) 1881.
30. Singh A.K., Quraishi M.A., *Corros. Sci.* 52 (2010) 152.
31. Srimathi M., Rajalakshmi R., Subhashini S., *Arab. J. Chem.* DOI:10.1016/j.arabjc.2010.11.013.
32. Markhali B.P., Naderi R., Mahdavian M., Sayebani M., Arman S.Y., *Corros. Sci.* 75 (2013) 269.
33. Yan Y., Li W., Cai L., Hou B., *Electrochim. Acta.* 53 (2008) 5953.
34. Joseph Raj X., Rajendran N., *Int. J. Electrochem. Sci.* 6 (2011) 348.
35. Ahamad I., Prasad R., Quraishi M.A., *J. Solid State Electrochem.* 14 (2010) 2095.
36. Lowmunkhong P., Ungthararak D., Sutthivaiyakit P., *Corros. Sci.* 52 (2010) 30.
37. Weihua L., Qiao H., Changlin P., Baorong H., *Electrochim. Acta.* 52 (2007) 6386.
38. Gopiraman M., Sathya C., Vivekananthan S., Kesavan D., Sulochana N., *J. Mater. Eng. Perform.* 21 (2012) 240.
39. Avci G., *Colloids and surface A: Physicochem. Eng. Aspects.* 317 (2008) 730.
40. Zhang Q.B , Hua Y.X, *Mater. Chem. Phy.* 119 (2010) 57.
41. Uwah I.E., Okafor P.C., Ebiekpe V.E., *Arab. J. Chem.* 6 (2013) 285.
42. Popoola A.P.I., Abdulwahab M., Fayomi O.S.I., *Int. J. Electrochem. Sci.* 7 (2012) 5805.
43. Anne Pauline S., Rajendran N., *Appl. Surf. Sci.* 290 (2014) 448.
44. Joseph Raj X., Nanjundan S., Rajendran N., *Ind. Eng. Chem. Res.* 51 (2012) 30.
45. Khaled K. F., *Appl. Surf. Sci.* 255 (2008) 1811.

46. Zhang F., Tang Y., Cao Z., Jig W., Wu Z., Chen Y., *Corros. Sci.* 61 (2012) 1.
47. Xu B., Liu Y., Yin X., Yang W., Chen Y., *Corros. Sci.* 74 (2013) 206.
48. Hmamou D.B., Salghi R., Zarrouk A., Aouad M.R., Benali O., Zarrok H., Messali M., Hammouti B., Kabanda M.M., Bouachrine M., *Ind. Eng. Chem. Res.* 52 (2013) 14315.
49. Obi Egbedi N.O., Obot I.B., *Arab. J. Chem.* 5 (2012) 121.
50. Khaled K.F., Al-Qahtani M.M., *Mater. Chem. Phy.* 113 (2009) 150.
51. Mahmoud N. El-Haddad, Fouda A.S., *J. Mol. Liq.*, 209 (2015) 480-486.
52. Yadav M., Behera D., Kumar S., Ranjan Sinha R., *Ind. Eng. Chem. Res.*, 52 (2013) 6318.
53. Zhang S., Tao Z., Li W., Hou B., *App. Surf. Sci.*, 255 (2009) 6757.
54. Chen S., He B., Liu Y., Wang Y., Zhu J., *Int. J. Electrochem. Sci.*, 9 (2014) 5400.
55. Bhrara K., Kim H., Singh G., *Corros. Sci.* 50 (2008) 2747.
56. Prabakaran M., Venkatesh M., Ramesh S., Periasamy V., *Appl. Surf. Sci.* 276 (2013) 592.
57. Lucero D.G., Xometl O.O., Palou R.M., Likhanova N.V., Dominguez Aguilar M.A., Febles V.G., *Ind. Eng. Chem. Res.* 50 (2011) 7129.
58. Shukla S.K., Quraishi M.A., *Mater. Chem. Phy.* 120 (2010) 142.

(2016) ; <http://www.jmaterenvironsci.com>